Dynamic Radar Cross Section Measurements of a Full-scale Aircraft for RCS Modelling Validation

R.F. van Schalkwyk and J.C. Smit

Radar and Electronic Warfare
CSIR DPSS
Pretoria, South Africa
rvschalkwyk@csir.co.za

Keywords: Radar Cross Section, Validation, Dynamic Measurements, Computational Electromagnetics.

Abstract

In this paper the process followed in generating a high fidelity reference data set for radar cross section (RCS) modelling validation for a full-scale aircraft, is presented. An overview of two dynamic RCS measurement campaigns, involving both single and stepped frequency operation, is provided and specific attention is given to calibration and the use of multi-bin stepped frequency processing for such measurements. Some of the challenges are noted and a preliminary comparison between the measured and calculated high range resolution profiles is presented. The results show that the data are of sufficient quality to enable future RCS modelling validation work.

1 Introduction

Radar cross section (RCS) modelling and simulation can contribute significantly towards various applications in radar and electronic warfare engineering, e.g. the generation of radar target signature databases for non-cooperative target recognition. The role of RCS modelling ranges from augmenting sparsely measured data sets to generating data sets for targets where measurements are not feasible. The value of calculated RCS data, however, strongly depends on the level of confidence in the accuracy of the results.

Validating both the computational electromagnetics (CEM) method(s) employed and the electromagnetic representation, i.e. computer aided design (CAD) model, of the object is important when qualifying the level of confidence in calculated results. This can be achieved using self-referencing or comparison with external reference data obtained through, for example, measurements [1].

RCS measurements of full-scale aircraft are usually obtained using static [2] or dynamic measurement configurations [3, 4], however, the inherent assumption of controlled access to the targets of interest may prove unrealistic when considering applications such as target classification database generation.

Further, in certain cases dynamic measurements may be the only way to measure target(s) of interest. This may be due to:

1. Target size and weight exceeding range specification [5].
2. Requirement to measure in relevant environment(s), e.g. ship in maritime environment [6] or aircraft undergoing in-flight deformation(s) and/or vibration [3].
3. Necessity to utilise existing radar(s) [3] (provided that suitable data recording and calibration is possible).

When high quality measured data are available, measurement based validation can be used to improve an RCS modelling capability through the development of insights into the mechanisms causing disparities between measured and calculated signatures. These insights can be used to improve either the RCS modelling process (e.g. refining the CAD model) or improving the measurement process (e.g. reducing measurement uncertainty). Such insights can thus enable the application of the modelling process with confidence to cases where measurements are not feasible and self-referencing validation processes are required.

The use of dynamic RCS measurements of civilian aircraft to obtain high fidelity reference data for future RCS modelling validation is explored in this paper. Some considerations derived from planned future validation work and the influence on the measurement requirements are presented. An X-band monopulse measurement radar facility was utilised to record raw aircraft return data, which was then processed to produce calibrated dynamic RCS measurements. The results presented here are initial examples of outputs from two measurement campaigns conducted using an Atlas Angel and a Cessna 182.

2 Requirements and Considerations

In the validation of the RCS modelling capability at CSIR, canonical and benchmark radar objects are used as far as possible to validate CEM methods and tools. However, in order to assess the applicability to electrically large complex structures such as aircraft, full-scale measurement validation becomes necessary. At present, the scope of validation is limited to aircraft for which the assumption of a perfect electric conductor (PEC) surface is reasonable. This assumption also reduces the complexity of the CEM validation in general given that more benchmark target results are available in open literature. The challenge of generating accurate CAD models of the targets is also reduced (in principle) to accurately capturing the shape of the exterior.

In order to obtain suitable RCS measurements that will facilitate both trend (e.g. mean RCS vs. aspect angle) as well

as feature (e.g. peak and null positions) based validation, a number of additional factors need to be considered.

2.1 Signature Characteristics vs Aspect Angle

The flight profile and waveform configuration(s) are two important factors that need to be considered when addressing aspect angle specific validation requirements. The angular rates (of the aircraft attitude relative to the radar sight line) and the pulse- or burst repetition frequencies will influence both the overall angular coverage and the angular spacing between RCS samples. This is important given that the available flight time imposes a trade-off between achievable coverage (in azimuth and elevation), angular resolution and revisit rate (i.e. repeated measurements at the same angle); each of which are important in the validation process.

Given the above, accurate knowledge of the target attitude information (i.e. roll, pitch and yaw) for each measurement sample is required. This could be derived from the measured radar positional data [7], however, the accuracy of this approach is limited and affected by environmental conditions. When available, time-synchronised attitude information can be obtained from an on-board inertial navigation system [5].

2.1.2 Range Resolution and Frequency

The ability to resolve scattering contributions from closely spaced physical features on the aircraft is an important requirement in feature-based validation. This requires high measurement resolution that can be achieved using wide bandwidth techniques such as stretched processing or stepped frequency waveforms.

2.1.3 Dynamic Range and Accuracy

A high spurious free dynamic range (SFDR) is required to identify small scatterers near large ones. This also facilitates the selection of a higher value for the minimum useful signal (10 to 20 dB SNR) [5]. A larger minimum useful signal is important to prevent measurement noise degrading accuracy when measuring small scatterers. A number of other factors can also affect the resulting accuracy e.g., reference source accuracy and linearity or drift in the system response.

3 Measurement Setup

RCS measurement campaigns were conducted several months apart at two different sites, using the same radar system. Similar processes were followed in both cases with only minor site-specific modifications. The campaign spanned a total of four days of measurements (excluding setup and testing time) and included two civilian aircraft, namely an Atlas Angel and a Cessna 182.

3.2 Calibration Setup

The calibration setup comprised a high precision 6 in. metal radar calibration sphere (with RCS of -17.4 dBsm) suspended from a Helikite using thin nylon rope. A diagram of the setup is shown in Figure 1.

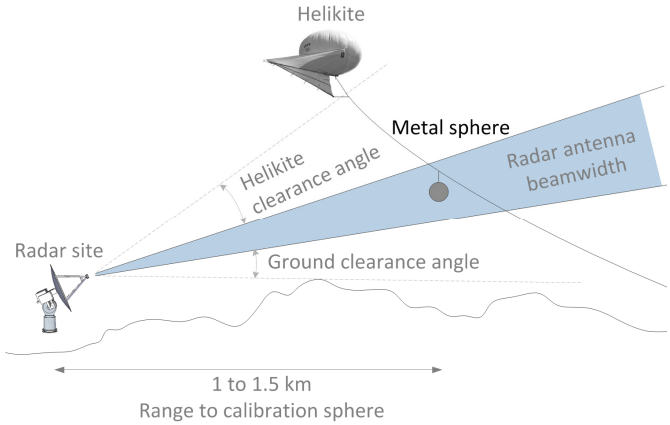

Figure 1: Calibration setup comprising Helikite and sphere.

Sphere measurements were conducted before and after each flight to enable compensating for drift in the system response. The dynamic range of the system was also verified using the calibration setup. The linearity and compression points of the RF front end were verified and the setup was fine-tuned until a repeatability error of better than 1 dB was achieved.

3.2 Aircraft

Both aircraft were fitted with a GPS aided attitude and heading reference system (AHRS). This system was mounted on a base plate and secured to the seat rails of the aircraft. The base plate was designed to ensure repeatable accurate alignment relative to the airframe. The location and attitude data was logged and stored for offline processing. The reported attitude accuracy of the solution varied from approximately 0.1° to 0.2°. Ideally, accuracies of 0.02° to 0.04° would be required to facilitate fine sampling of the aircrafts' inherent RCS lobing pattern.

Flight profiles facilitating both angular diversity and un-aliased sampling of the RCS lobing pattern were selected. An example of measured flight profile data is shown in Figure 2.

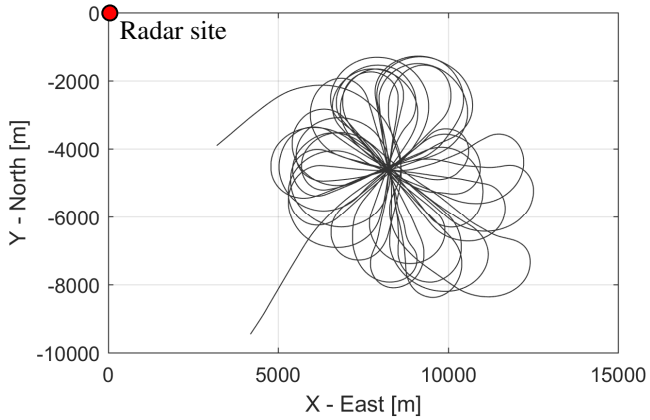

Figure 2: Atlas Angel flight profile (day 1).

The "flower pattern" flight profile results in a combination of high angular rates during turns (approximately 180° per minute) and low angular rates during crossing legs. During

the tangential crossing legs, the pilot was requested to perform significant wing rock (banking up to 60°). This was done in order to increase elevation aspect angle coverage and should allow for the generation of ISAR images in elevation.

3.3 Radar

The radar was configured to track and record in either single frequency pulse-Doppler or stepped frequency modes. The radar parameters used are presented in Table 1.

Radar Parameter	*Value*
Frequency band	X-band
PRF	10 KHz
Bandwidth Single frequency Stepped FM	 40 MHz 1.28 GHz
Number of pulses	64

Table 1: Radar parameters used in measurements.

A range resolution of approximately 15 cm was obtained using the total measured bandwidth. In stepped frequency mode a 50% spectral overlap between consecutive pulses was used to ease stepped frequency processing [8]. The burst repetition frequency (BRF) of 156 Hz resulted in angular sampling increments of 0.02° at the highest angular turn rate of approximately 180° per minute.

4 Data Processing and Analysis

Post-trial data processing included deriving observed target aspect angles from the AHRS data, extracting equalisation and calibration coefficients from the calibration measurements (vs. frequency and attenuation) and generation of calibrated HRR profiles. Simulated RCS data of the aircraft was also generated for initial comparison.

4.1 Calibration Data

An iterative process was followed in deriving the complex equalisation and calibration coefficients required for stepped frequency processing, due to challenges associated with the dynamic RCS measurement process. Challenges included high sidelobes due to spectral "stitching" when using only measurement derived positional based motion compensation, clutter contamination (when the Helikite lost altitude due to wind gusts) and contamination from small birds and insects. A short sequence of consecutive HRR profiles of the sphere, calibrated using only radar range measurement based motion compensation is shown in Figure 3. Stitching sidelobes can be seen at integer multiples of 7.5m – which corresponds to the range ambiguity associated with frequency steps of 20 MHz – with an insect flying (from 5m to 15m) visible in the data.

During the data analysis a technique was developed that iteratively minimises the energy at the expected stitching side lobe locations through fine phase matching. This produced much improved results for both the calibration sphere and aircraft measurements. It was also established that Doppler processing can (in certain instances) be used to suppress the contamination from clutter and insects.

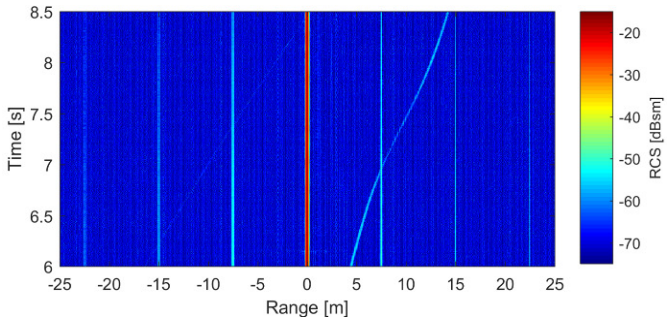

Figure 3: Sequence of HRR profiles of the calibration sphere with only range measurement based motion compensation.

An HRR profile of the calibration sphere, calibrated using the fine phase matching technique discussed above (with no clutter or insects present), is presented in Figure 4. The result shows an SFDR between 45 and 50 dB being achieved.

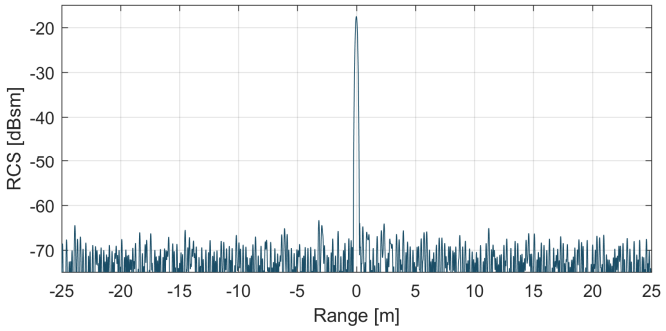

Figure 4: Multi-bin HRR profile of the calibration sphere with fine motion compensation calibration applied.

4.2 Aircraft Data

The observed target aspect angles were derived from the recorded attitude and positional data. A combination of GPS time stamping and correlation was used to align the attitude and RCS data. Coarse motion compensation based on the recorded platform data was applied, followed by the fine motion compensation technique developed using the calibration data. Comparative multi-bin HRR profiles for the Atlas Angel, broadside and banking during a turn, is shown in Figure 5.

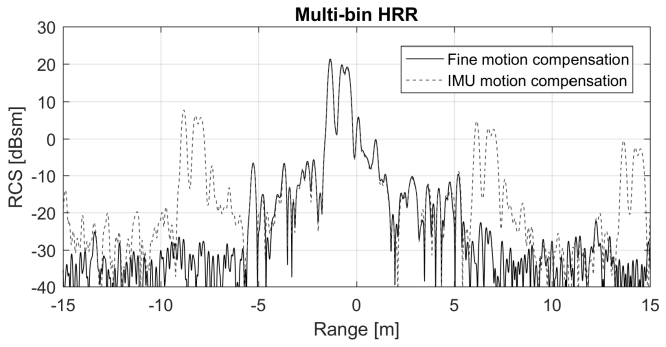

Figure 5: Multi-bin HRR profile of Atlas Angel with coarse and fine motion compensation calibration applied.

A limitation when using stepped frequency waveforms is the low BRF, which causes micro-Doppler from the propeller to be ambiguous. This was observed in the data and degraded performance of fine motion compensation when the propeller scattering contribution was significant. Despite small sections of data being affected by this limitation, most of the data are of sufficient quality to be used for fairly detailed RCS modelling validation comparisons.

4.3 Modelling and Simulation

A high fidelity CAD model, constructed using laser scanned point cloud data of the specific Atlas Angel aircraft used for the RCS measurements, was developed. This model, shown in Figure 6(a), and the SigmaHat RCS calculation software [9], was used to generate simulated RCS data for comparison with the measured data.

Initial RCS calculations were performed spanning the aspect angles covered in the measurements (at 0.1° and 0.5° increments in azimuth and elevation respectively). This data set was used as reference to determine the alignment between the AHRS and aircraft coordinate systems. To achieve this, the measured aspect angles, as derived from the AHRS, were used to interpolate the calculated matrix of RCS vs angle data. The angular offsets between the dominant localised scattering features in the calculated and measured RCS data were then used to characterise the AHRS-aircraft alignment.

The calculated RCS values used in the comparisons were generated using aspect angles derived from the AHRS as direct inputs into SigmaHat to avoid any interpolation errors.

4.4 Comparison (Measured vs. Calculated)

In order to demonstrate the usefulness of the measured RCS data, a comparison between the measured and calculated HRR RCS values over a small window of aspect angles was performed. In this subset of the data, the aircraft is turning with a bank angle of approximately 20° with the nose pointed directly at the radar at the 0° azimuth aspect angle. The measured HRR RCS profiles are shown in Figure 6(b). The calculated HRR RCS profiles generated using the CAD model originally developed for this investigation (hereafter referred to as the base CAD model) – with a stationary propeller – is shown in Figure 6(c). The HRR RCS profiles for the modified CAD model (as discussed in Section 4.4.1) – with a rotating propeller – is shown in Figure 6(d).

Comparison of Figure 6(b) and 6(c) using visual inspection highlights several areas of both good and poor agreement. Direct comparison of the range profiles with the CAD model, using Figure 6(a), allows for association of the scattering contributions with specific geometrical features on the aircraft. Some notable areas of good agreement include:

1. Location and structure of the scattering associated with the front, middle and tail of the aircraft.
2. Location of the horizontal stabiliser flash (-8° at 3.1m).

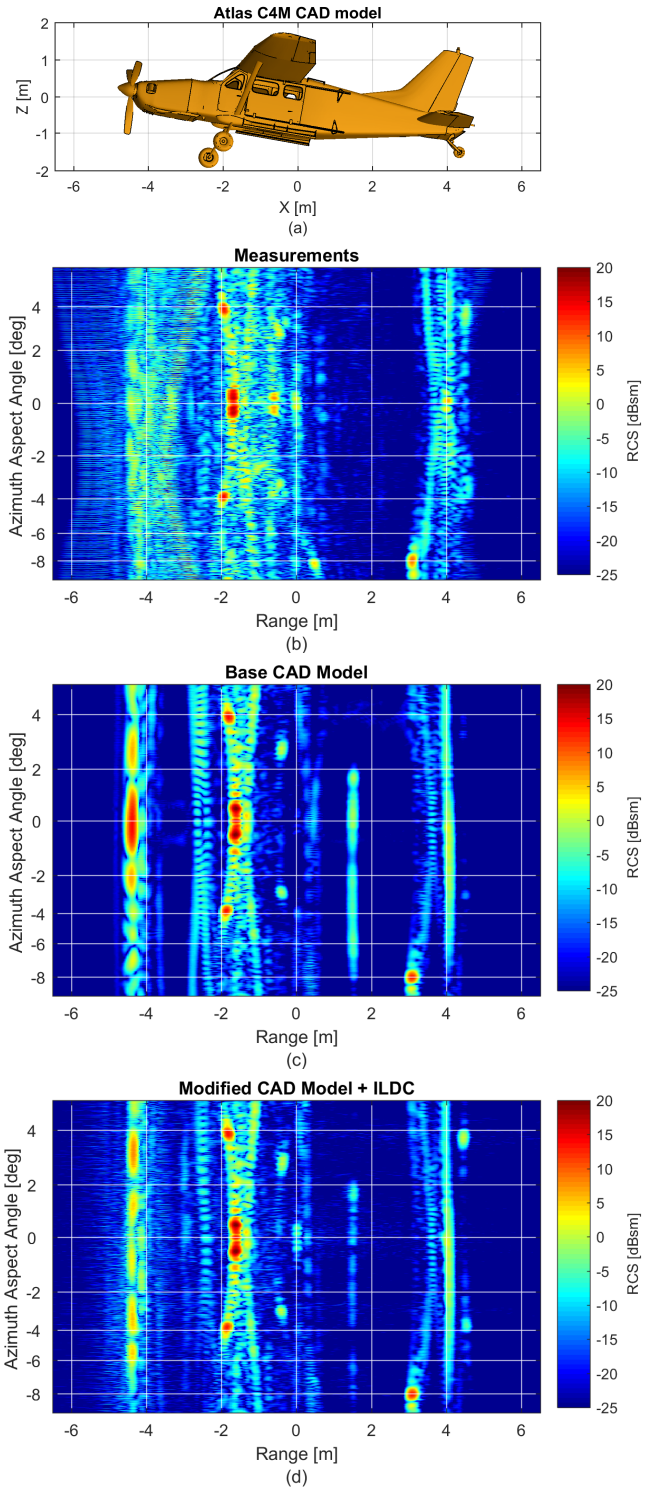

Figure 6: a) 3D CAD model of the Atlas Angel aircraft with a comparison of HRR RCS profiles as a function of azimuth aspect angle between b) measured reference c) calculated (using the base CAD model), and d) calculated (using the modified CAD model with ILDC and rotating propeller).

3. Location and amplitude of the wing flashes:
    a. ± 0.2° at -1.6m,
    b. ± 4° at -1.8m (tapered outer of wing).

Some notable areas of disagreement include.

1. More low amplitude scattering observed in the measurements between the propeller and trailing edge of the wings (-4.5m to 0m).
2. Localised scattering not present in the calculated results:
    a. ± 0.2° at -0.6m and 0m (trailing edge of wings),
    b. ± 3.8° at 4.5m (location of elevators).
3. Stronger scattering at the front of the aircraft in the calculated results (-4.4m).
4. Scattering from the rear of the cabin (1.5 m) observed only in the calculations.
5. More persistent scattering from the tail wheel (4m) observed in the calculated results.
6. Scattering from the propeller spread in range in the measurements.

4.4.1 Model Refinement

In order to both understand and reduce some of the areas of disagreement observed between Figure 6(b) and 6(c), an iterative approach of model refinement was followed. The calculated HRR RCS profiles from the refined model is shown in Figure 6(d).

Factors addressed in the model refinement include:

1. Rotation of the propeller during the simulation.
2. The PEC surface at the rear of the empty cabin was replaced with idealised absorber. This was included as a first order compensation for the very complex (but lossy) dielectric interactions occurring inside the cabin involving humans, seats, etc.
3. The PEC surface of the wheels was replaced with an idealised -20 dB absorbing surface.
4. Features missing on the nose of the base CAD model (air intake and indented regions around the adjacent holes) were included as shown in Figure 7.
5. SigmaHat's incremental length diffraction coefficient (ILDC) method was enabled to better account for scattering contributions from edges.

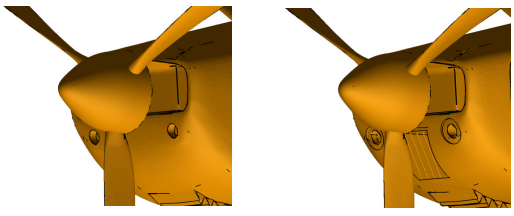

(a) (b)

Figure 7: Zoomed view of the noise of the a) base and b) modified CAD models of the Atlas Angel.

4.4.2 Improved Results

Visual inspection of the calculated HRR RCS profiles for the modified CAD model, with rotating propeller and ILDC enabled, as shown in Figure 6(d), show clear improvements compared to the results for the base CAD model. The improvements include:

1. Similar (albeit lower amplitude) scattering characteristics from the propeller as observed in the measurements.
2. Reduction of the scattering from the rear of the cabin (1.5m).
3. More consistent lower amplitude scattering from the front of the aircraft compared to the measurements.
4. Presence of localised scattering from the trailing edges of the wings (0m) and elevators (4.5m).

The improvements can also observed when comparing single frequency RCS vs. aspect angle results for the calculated and measured data. An example for 8.8 GHz is shown in Figure 8.

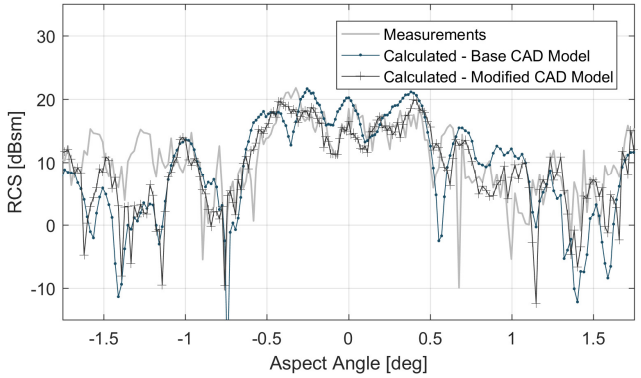

Figure 8: Calculated and measured RCS of the Atlas Angel observed over 3 degrees aspect angle at 8.8 GHz.

The feature selective validation (FSV) method, proposed in [10], was used to quantify the improvement gained using the modified CAD model. The method decomposes the input and reference data into amplitude (slow variations) and feature (sharp peaks and transitions) data sets. The sample-to-sample agreement is then quantified through the use of two difference measures, namely the amplitude difference measure (ADM) and feature difference measure (FDM) respectively. These two measures are weighted and combined to obtain a global difference measure (GDM), which is an overall goodness-of-fit between the two data sets. It is important to note that the FSV measures quantify the differences between the input and reference data and lower output values, therefore, correspond to higher levels of agreement.

The results of an FSV comparison for the data set shown in Figure 8 are presented in Figure 9. The confidence histograms show significant improvement in the amplitude of the results (as per ADM) with slight improvement in the features (as per FDM). The GDM shows an overall improvement in the level of agreement with the GDM mean value improving from 0.96 (using the base CAD model) to 0.71 (using the modified CAD model).

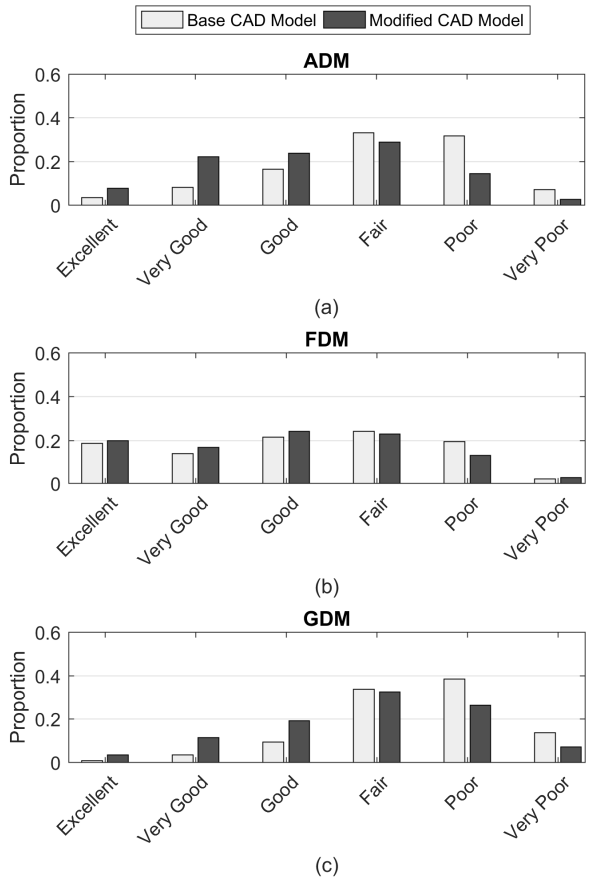

Figure 9: Confidence histograms (ADM, FDM and GDM) comparing the agreement between the calculated (base and modified CAD models) and measured RCS data of the Atlas Angel at 8.8 GHz.

5 Conclusions

In this paper both the process followed as well as preliminary results from two dynamic RCS measurement campaigns of a full-scale civilian aircraft, were presented. The goal of the campaigns was to obtain high fidelity reference data suitable for performing RCS modelling validation. Some of the important factors that need to be taken into account in the generation and processing of such data were considered. The SFDR achieved (on most of the data) and the level of agreement with calculated RCS results (based on qualitative visual comparison and quantitative comparison using the FSV method) highlights that the data are of sufficient quality to be used for future RCS validation work. It has also been illustrated that by comparing measured and calculated results and applying model refinements in an iterative manner, significantly improved calculated RCS results for a full-scale civilian aircraft can be obtained, even when using asymptotic CEM methods.

Acknowledgements

The authors would like to thank the members of CSIR DPSS's Experimental Radar Systems team for their assistance during the RCS measurement campaigns. This work was funded by the Armaments Corporation of South Africa SOC Ltd. (ARMSCOR) through its Electronic Defence Evaluation and Research Institute (EDERI) technology funding programme.

References

[1] *IEEE Standard for Validation of Computational Electromagnetics Computer Modeling and Simulations*, IEEE STD 1597.1-2008, 2008.

[2] J. W. Odendaal, L. Botha and J. Joubert. "A full-scale static radar cross-section (RCS) measurement facility," *South African Journal of Science*, Vol.103, pp. 196-198, 2007.

[3] I. D. Olin and F. D. Queen, "Dynamic measurement of radar cross section," *Proc. IEEE*, Vol. 53, pp. 954-961, 1965.

[4] A. Jain, I. Patel, "Dynamic imaging and RCS measurements of aircraft," *Aerospace and Electronic Systems IEEE Transactions on*, vol. 31, pp. 211-226, 1995.

[5] *IEEE Recommended practice for Radar Cross –Section Test Procedures*, IEEE STD 1502-2007, 2007.

[6] T. E. Tice, "An overview of radar cross section measurment techniques," *IEEE Trans. Instrum. Meas.*, vol. 39, no. 1, pp. 205-207, Feb. 1990.

[7] W. D. Caraway and D. C. Abell, "A method for the determination of target aspect angle with respect to a radar," U.S. Army Missile Command, Alabama, Tech. Rep. RD-MG-96-32, 1996.

[8] A. J. Wilkinson, R. T. Lord, and M. R. Inggs, "Stepped-frequency processing by reconstruction of target reflectivity spectrum," *Proc. IEEE South African Symp. Commun. Signal Process. (COMSIG)*, pp. 101–104, 1998.

[9] J. C. Smit, "SigmaHat: A toolkit for RCS signature studies of electrically large complex objects," *IEEE Radar Conference 2015*, pp 446-451, 2015.

[10] A. P. Duffy, A. J. M. Martin, A. Orlandi, G. Antonini, T. M. Benson, and M. S. Wolfson, "Feature selective validation of computational electronics(CEM), Part I—The FSV method," *IEEE Trans. Electromagn. Compat.*, vol. 48, no. 3, pp. 449–459, Aug. 2006.